ANN MODELING FOR GREY PARTICLES PRODUCED FROM INTERACTIONS OF DIFFERENT PROJECTILES WITH EMULSION NUCLEI AT 4.5 AGEV/C.

M.N. Yasein El-Bakry[1], A.M. Basha[1], N. Rashed[1], A. Radi[2], M.A. Mahmoud[1]

1 physics department, faculty of Science, Fayoum University, Egypt.
2 physics department, faculty of Science, Ain Shams University, Egypt.

Abstract

Artificial Neural Network (ANN) is one of the important tools in high energy physics. In this paper, we are using ANN for modeling the multiplicity distributions of grey particles produced from interactions of P, ^{3}He, ^{4}He, ^{6}Li, ^{12}C, ^{24}Mg, and ^{32}S with emulsion nuclei, light nuclei (CNO), and heavy nuclei (AgBr). The equations of these distributions were obtained.

Keywords: *"Artificial Neural Network", "Nuclear emulsion", "Light nuclei (CNO)", and "Heavy nuclei (AgBr)".*

1- INTRODUCTION

Multiparticle production and multifragment emission are important experimental phenomena in high energy collisions [1, 2]. They are providing vital information about the nuclear reaction mechanism.

According to the participant-spectator model [3], the nuclear interacting system in high energy nucleus-nucleus collisions can be divided into three parts: a projectile spectator, a participant, and target spectator. The overlapping part of two colliding nuclei is called participant and the other parts are called the target spectator and the projectile spectator, respectively.

The projectile spectator region: is characterized by small momentum transferred that is enough to dissociate the projectile into few fragments moving in the forward direction or scattered by relatively small angle. Simple elastic scattering [4] assuming optical potential [5], diffraction [6] and Coulomb dissociation [7] models are sufficient to describe the fragmentation process and the angular spread of the emitted fragments in this region.

The target spectator region: The nucleons in this region are initially at rest. As the collision starts up, nucleons from the projectile defuse slowly through the target transferring a little bit fraction of the projectile energy. The diffusion rate depends mainly on the impact parameter. The system then behaves as perfect gas that suffers multiple of successive elastic scattering. Consequently the entropy of the system increases until it reaches equilibrium state, with equilibrium temperature of the order of 30 MeV. At this moment the system evaporates [8] producing heavily ionizing fragments appear as black particles with isotropic distribution in the space. In most cases it was sufficient to describe the energy distribution of the evaporated particles with a unique Maxwell distribution of classical distinguished particles.

The hot spot region: The overlap region between the projectile and the target is the hottest region in the space. Large amount of heat is dissipated there. The nuclear matter goes through different stages. In the early one a sudden compression occurs to the nuclear matter accompanied by much increase in matter density and production of large amount of center of mass energy. The environment is now adequate for the formation of quark-gluon plasma phase [9]. Many quarks-antiquarks are being created followed by a recombination process. The created quark pairs form what are called sea quarks. Neighboring quark-antiquark may recombine again forming meson [10]. Successive collisions go on producing more newly created particles and hence the system expands again until the collisions cease. If we treat the system thermodynamically [11], it is expected that fast light particles be produced in the early stage in the forward direction. As time goes up, the system is subjected to successive collisions each of them followed by creation of bunches of newly produced particles that emitted in wider emission angle. Finally the nucleons 3 are emitted individually or rather in cluster or fragment form. The singly charged fragments are produced as knocked on nucleons with medium energy range ($26\ MeV < E < 400\ MeV$) and appear in emulsion plates as gray particles [12]. In the present work we use the neural network for modeling of multiplicity distributions of this type of particles (grey particle).

2- METHOD OF TARGET IDENTIFICATION

The exact target identification in an emulsion experiment is not possible as the medium is composed of various elements as mentioned in table (1). However, we can divide the major constituent elements into three broad groups such as H, CNO, and AgBr with high accuracy. There are a lot of other ways of statistical separation [13-17], which roughly give the probability of interactions with different targets. It well known that the number of heavy particles, N_h is a good tool for target identification [18]. Since we are interested in the separation of targets on event-by-event basis, we have attempted the separation of targets using the following criteria:

1. The group of events at ($N_h = 0, 1$) represents the interactions with a free Hydrogen (H) in addition to those events due to electromagnetic dissociations of the projectile ions which are characterized by ($N_h = 8,\ n_s = 0$) [19, 20].
2. The group of events having ($2 \le N_h \le 8$) represented the interaction with (CNO) group in addition to peripheral collision (AgBr). Using the Florian method [21] one can separate the number of events due to (CNO) and that due to (AgBr) individually, from the sample of event having ($2 \le N_h \le 8$).
3. All events having $N_h \ge 9$ represented the interactions with (AgBr). From these events. It can be found that the events belonging to the complete destruction of (AgBr) nuclei are distinguished by $N_h \ge 28$ [22].

Table (1): The chemical composition of BR-2 emulsion

Element	^{1}H	^{12}C	^{14}N	^{16}O	^{80}Br	^{108}Ag
No of atoms/cc X $^{22}10$	3.150	1.410	0.395	0.956	1.028	1.028

3- ARTIFICIAL NEURAL NETWORK

An ANN is made up of a number of simple and highly interconnected computational elements. There are many types of ANNs, but all of them have three things in common: individual neurons (processing elements), connections, and learning algorithm. The processing element calculates the neuron transfer function of summation of weighted inputs. A simple neuron structure is shown in Fig (1). A network consists of one or more layers of neurons. A layer of neurons is a number of parallel neurons. Any network consists of three parts; input layer, number of hidden layers, and output layer.

In mathematical term, we may describe a neuron K by writing the following equation:

$$Y_k = f(\sum_{j=1}^{m} W_{kj} x_j + b_k) \quad (1)$$

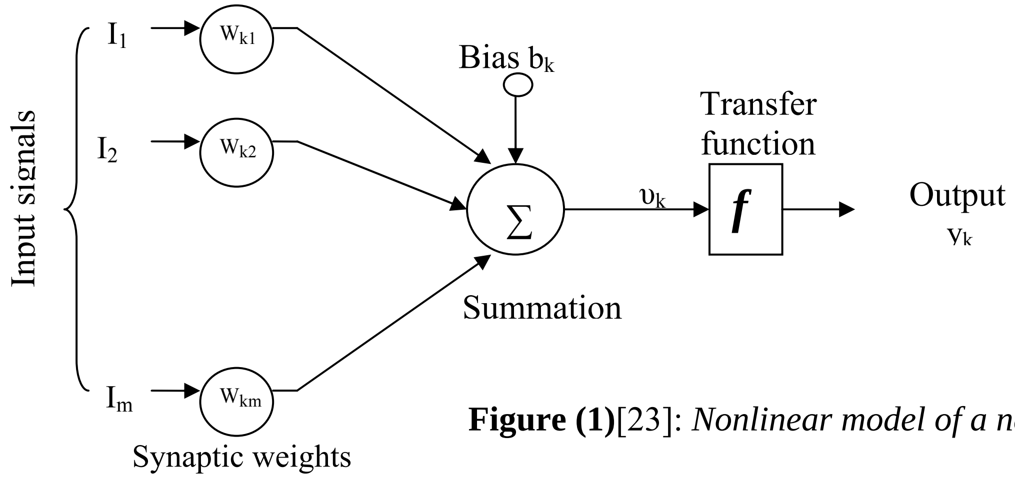

Figure (1)[23]: *Nonlinear model of a neuron.*

4- MODELING OF MULTIPLICITY DISTRIBUTION OF GRAY PARTICLES

The proposed neural network (ANN) model of multiplicity distributions of grey particles which produced from the interactions of P, ^{3}He, ^{4}He, ^{6}Li, ^{12}C, ^{24}Mg, and ^{32}S with emulsion nuclei at the whole, group of light nuclei (CNO), and group of heavy nuclei (AgBr) is a two inputs and one output. The first input is the mass number "A" of projectile nuclei = 1, 3, 4, 6, 12, 24 and 32, the second input is the number of grey particles N_g. The output is the probability of charged particles P (N_g).

Using this input output arrangements different network configurations were tried to achieve good mean square error (mse) and good performance for network.

4.1- Interactions with emulsion nuclei

The proposed neural network model of multiplicity distributions for grey particles produced from the interactions of different projectiles and emulsion nuclei is two input (A, N_g) , one output [P(N_g)], and three hidden layers which consist of 8, 6, and 6 neurons. The configuration of proposed ANN model shown in figure (2). The transfer function of the first, second, and third hidden layers were chosen to be a ***tan sigmoid***, while the output was chosen to be ***pure line*** (see Appendices).

The proposed ANN in the present work was trained using Levenberg – Marquardt optimization technique [24, 25]. The optimization technique is more powerful than the conventional gradient descent technique.

The Levenberg – Marquardt updates the network weights using the following rule:

$$\Delta W = (2J^T J + \mu I)^{-1} 2J^T e \tag{2}$$

Where J is the Jacobian matrix , e is a vector of ANN errors, μ is scalar, changed adaptively by the algorithm, and *I* is identity matrix.

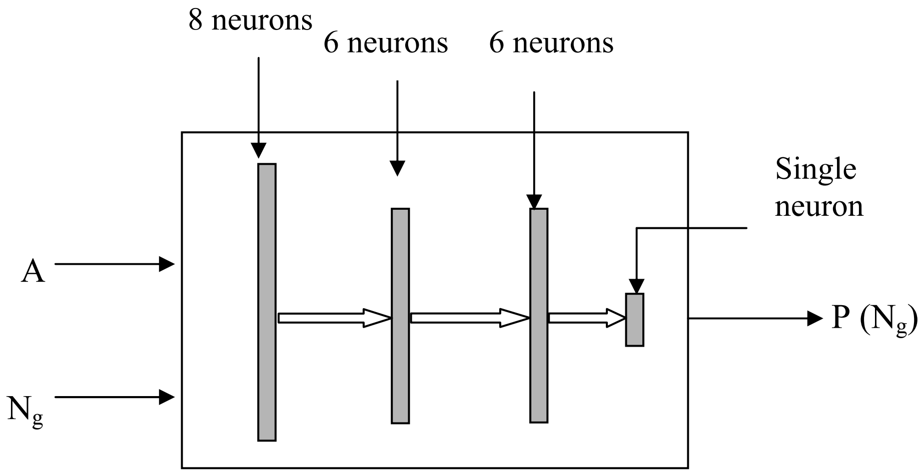

Figure (2): *A block diagram for different beams with emulsion nuclei based ANN model.*

The net which used in this is the feed forward neural network back propagation. The trained method which used to train the ANN model is Levenberg - Marquardt optimization technique, with learning rate = 0.15, number of epochs = 1000, and momentum = 0.2. In this case P, ^{4}He, ^{6}Li, ^{12}C, ^{24}Mg, and ^{32}S are used to trained neural network, after this training, we made ANN model to predict untrained data such that ^{3}He data as shown in figure (3). It can be seen from these figures that the trained and predicted neural network model shows almost exact fitting. The match is still good; indicating that designed ANN is robust. Table (2) shows the comparison between the average number of grey particles which obtained from experimental data and its average which obtained from output of ANN model.

Table (2): *Comparison between $<N_g>$ from experimental data and $<N_g>$ANN from ANN which produced from the interaction between different projectile and emulsion nuclei at 4.5 A GeV/c.*

projectile	$<N_g>$ experimental	$<N_g>$ ANN
P	1.758 ± 0.032	1.7584
^{3}He	2.532 ± 0.072	2.3551
^{4}He	2.581 ± 0.101	2.6060
^{6}Li	3.038 ± 0.094	3.0129
^{12}C	3.749 ±0.148	3.7547
^{24}Mg	4.314 ±0.223	4.3075
^{32}S	4.003 ± 0.168	3.9994

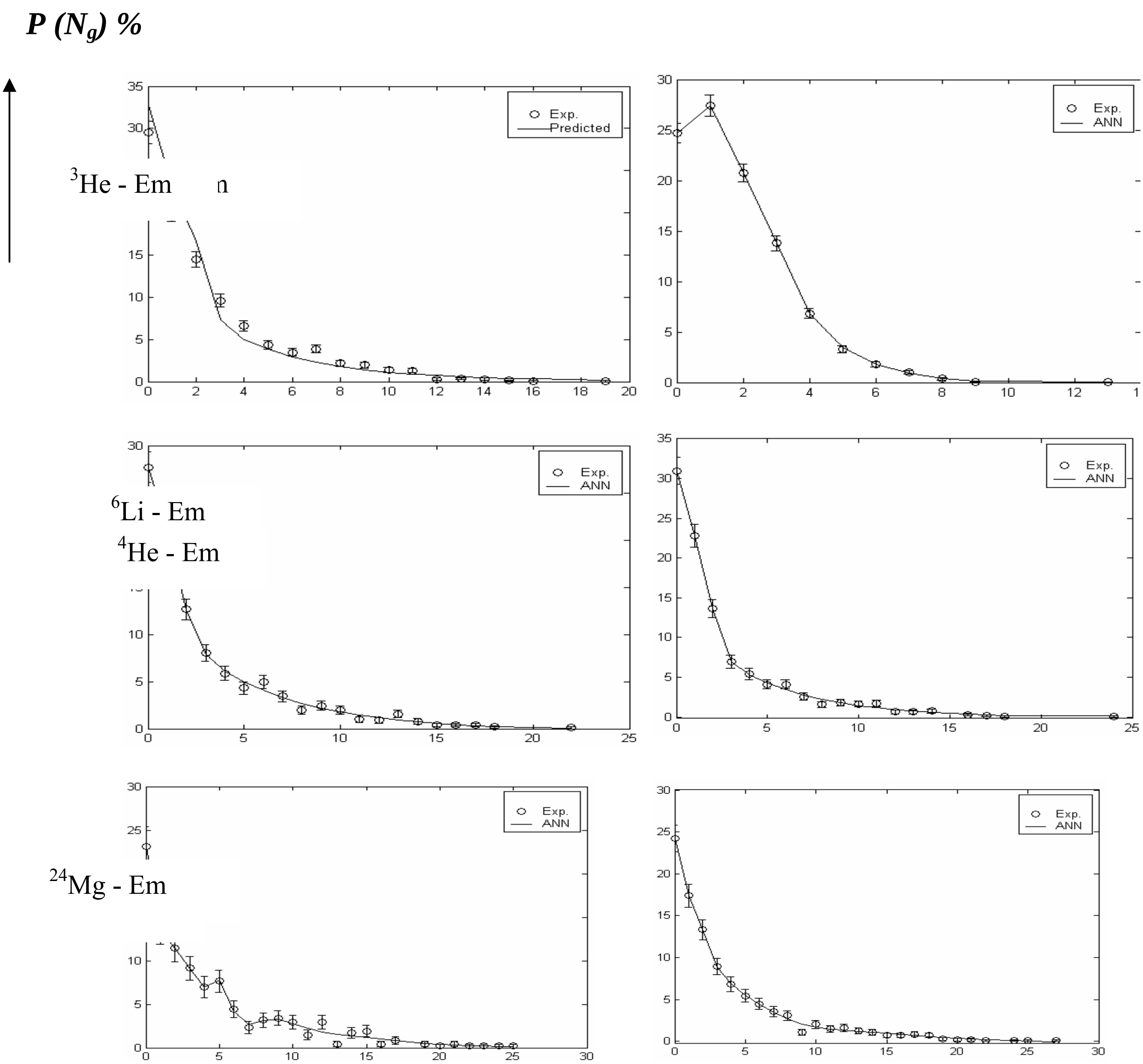

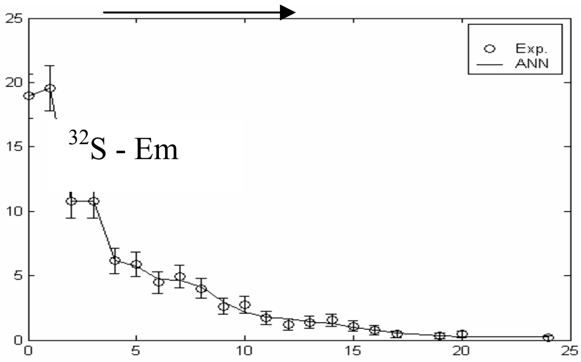

N_g

Figure (2): *Multiplicity Distributions of grey particles (N_g) as simulated by the neural network (trained and predicted data) for the interactions of different beams with emulsion nuclei at 4.5 A GeV/c [(O) Experimental data (-) ANN model].*

The multiplicity distributions of grey particles which produced from the interactions different beams with emulsion nuclei can be described by

$$P(N_g)_{Em} = \text{pur line}[(\text{net.LW}\{5,4\} \text{ tan sigmoid}(\text{net.LW}\{4,3\} (\text{tan sigmoid}(\text{net.LW}\{3,2\}(\text{tan sigmoid}(\text{net.LW}\{2,1\} (\text{pur line}(\text{net.IW}\{1,1\}A+\text{net.b}\{1\})+\text{net.b}\{2\}) +\text{net.b}\{3\})+\text{net.b}\{4\})+ \text{net.b}\{5\})] \quad (3)$$

The weights and biases in equation (3) are given in appendix A.

4.2- Interaction with light nuclei (CNO) group

The proposed neural network model of multiplicity distributions of grey particles which produced from the interactions of different projectiles with light nuclei (CNO) group in two inputs, three hidden layers, and one output is considered. The numbers of neurons in hidden layers are 9, 6, and 6 respectively. The transfer function of the first, second, and third hidden layers were chosen to be a ***tan sigmoid***, while the output was chosen to be ***pure line***.

The feed forward neural network back propagation is used to the modeling. The trained method which used to train the ANN model is Levenberg - Marquardt optimization technique, with learning rate = 0.091, number of epochs= 184, and momentum = 0.13. In this case P, ^{3}He, ^{6}Li, ^{12}C, ^{24}Mg, and ^{32}S are used to trained neural network, after this training, we made ANN model to predict untrained data such that ^{4}He data as shown in figure (3). It can be seen from these figures that the trained and predicted neural network model shows almost exact fitting. The match is still good; indicating that designed ANN is robust. Table (3) shows the comparison between the average number of grey particles which obtained from experimental data and its average which obtained from output of ANN model.

The function of these multiplicity distributions of grey particles which obtained from ANN model is

$$
\begin{aligned}
P(N_g)_{(CNO)} = & \text{pur line}[(\text{net.LW}\{5,4\}\ \text{tan sigmoid}(\text{net.LW}\{4,3\} \\
& (\text{tan sigmoid}(\text{net.LW}\{3,2\}(\text{tan sigmoid}(\text{net.LW}\{2,1\} \\
& (\text{pur line}(\text{net.IW}\{1,1\}A+\text{net.b}\{1\})+\text{net.b}\{2\}) \\
& +\text{net.b}\{3\})+\text{net.b}\{4\})+\text{net.b}\{5\}]
\end{aligned}
\tag{4}
$$

The values of the weights and biases are collected in appendix B.

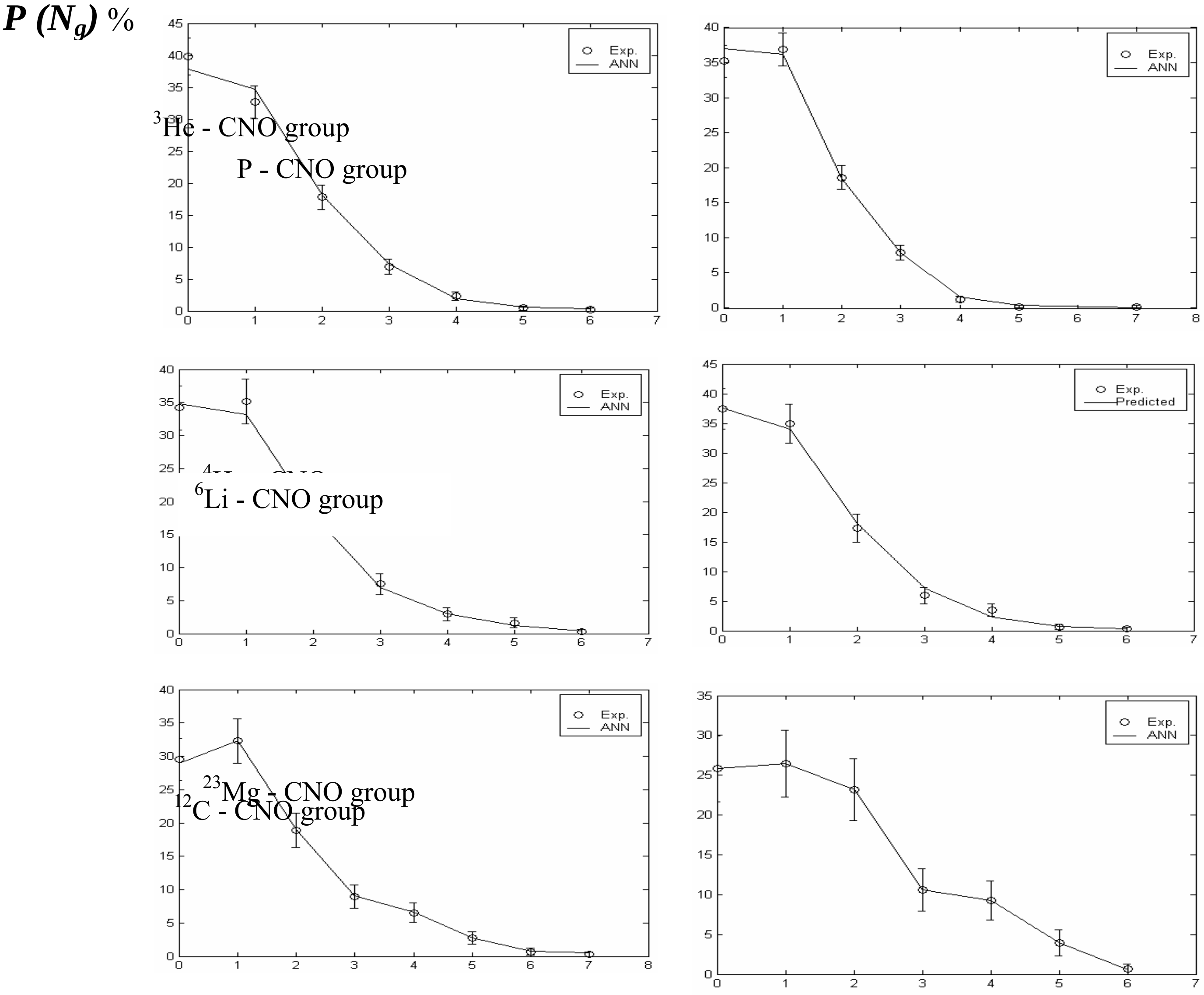

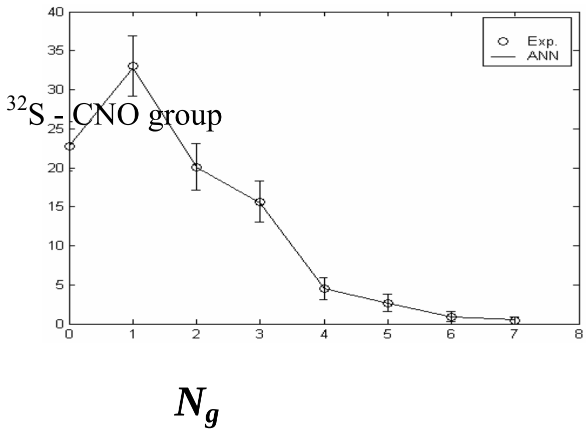

Figure (3): *Multiplicity Distributions of grey particles (N_g) as simulated by the neural network (trained and predicted data) for the interactions of different beams with light nuclei (CNO) group at 4.5 A GeV/c (O) Experimental data (-) ANN model.*

Table(3): *Comparison between <N_g> from experimental data and <N_g>ANN from ANN which produced from the interaction between different projectile and light nuclei (CNO) group at 4.5 A GeV/c.*

projectile	<N_g> experimental	<N_g> ANN
P	1.0423 ± 0.041	1.0401
^{3}He	1.0146 ± 0.046	1.0548
^{4}He	1.0629 ± 0.6	1.0638
^{6}Li	1.1596 ± 0.066	1.1049
^{12}C	1.4330 ± 0.084	1.4542
^{24}Mg	1.6556 ± 0.13	1.6488
^{32}S	1.5982 ± 0.11	1.5955

4.3- Interaction with heavy nuclei (AgBr) group

The proposed neural network model of multiplicity distributions of grey particles which produced from the interactions of P, ^{3}He, ^{4}He, ^{6}Li, ^{12}C, ^{24}Mg, and ^{32}S with heavy nuclei (AgBr) group is two inputs, three hidden layers, and one output. The hidden layers consist of 8, 6, and 6 neurons, the configuration of proposed ANN model shown in fig. (2). The transfer functions are chosen for first, second, and third hidden layers is ***log sigmoid***, but the transfer function for output is ***pure line***. The net which used in this is the feed forward neural network back propagation. The trained method which used to train the ANN model is Levenberg - Marquardt optimization technique, with learning rate = 0.15, number of epochs = 700, and momentum = 0.52.

Simulation results based on the ANN approach to modeling the multiplicity distributions of grey particles produced from P, ^{3}He, ^{4}He, ^{6}Li, ^{12}C, ^{24}Mg, and ^{32}S interactions with AgBr target nuclei at 4.5 A GeV/c are given in figure (4). It can be seen from these figures that the trained neural network model shows almost exact fitting. The match is still good; indicating that designed ANN is robust. Table (4), show the comparison between the average number of grey particles which obtain from experimental data and output of neural network.

The function of these multiplicity distributions of grey produced particles from the interactions of different projectiles with (AgBr) group which obtained from ANN model is

$$P(N_g)_{(AgBr)} = \text{pur line}[(\text{net.LW}\{5,4\}\ \text{log sigmoid}(\text{net.LW}\{4,3\}\ (\text{log sigmoid}(\text{net.LW}\{3,2\}(\text{log sigmoid}(\text{net.LW}\{2,1\}\ (\text{pur line}(\text{net.IW}\{1,1\}A+\text{net.b}\{1\})+\text{net.b}\{2\}) +\text{net.b}\{3\})+\text{net.b}\{4\})+ \text{net.b}\{5\}] \quad (5)$$

The values of the weights and biases are collected in appendix C.

P (N$_g$) %

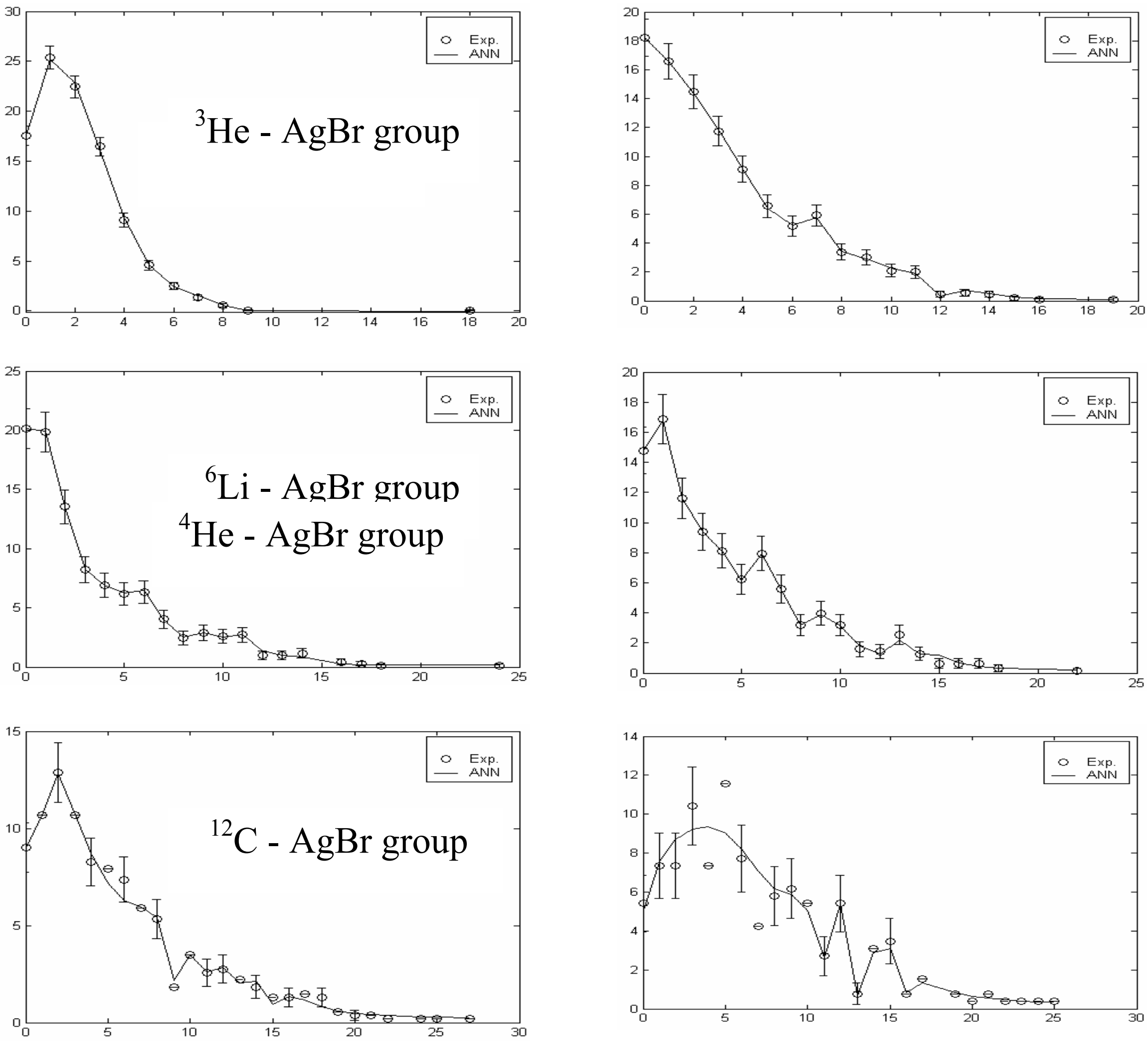

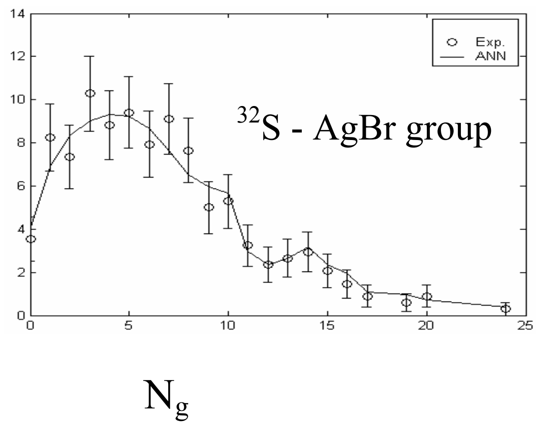

Figure (4): *Multiplicity Distributions of grey particles (N_g) as simulated by the neural network for the interactions of different beams with heavy nuclei (AgBr) group at 4.5 A GeV/c [(O) Experimental data (-) ANN model].*

Table (4): *Comparison between $<N_g>$ from experimental data and $<N_g>$ANN from ANN model which produced from the interaction between different projectiles and heavy nuclei (AgBr) group at 4.5 A GeV/c.*

projectile	$<N_g>$ experimental	$<N_g>$ ANN
P	2.0911±0.08	2.0798
^{3}He	3.4413±0.104	3.4641
^{4}He	3.5684±0.14	3.5427
^{6}Li	4.3657±0.17	4.3681
^{12}C	5.6783±0.25	5.6221
^{24}Mg	6.8610±0.43	6.8841
^{32}S	6.5147±0.35	6.6694

CONCLUSION

(1) Almost exact fitting for the grey particles produced from interactions of different projectiles with (Em, light nuclei CNO, and heavy nuclei AgBr).

(2) Not only simulated the trained observations but also predicted the multiplicity distributions for non trained observations.

(3) The capability of the ANN to simulate and predict the experimental observations with almost exact accuracy recommends the ANN to dominate the modeling techniques in high energy physics.

(4) The equations which describe the multiplicity distributions of grey particles can be obtained.

(5) The prediction in (A-A) is almost exact, but in (H-A) proved better matching with the experimental data. We owing this to the mechanism of the interaction between nucleus-nucleus.

APPENDICES

Sigmoid function $Y = \frac{1}{1+e^{-x}}$, pure line function $Y = X$

Appendix A

$$net.IW\{1,1\}=\begin{pmatrix} -0.0276 & 0.0220 \\ 0.0053 & -0.0503 \end{pmatrix} \qquad net.LW\{2,1\}=\begin{pmatrix} 2.6931 & 2.9030 \\ 2.9290 & 2.6651 \\ -0.6398 & -3.8640 \\ -3.9470 & -0.1039 \\ 1.2514 & 2.3824 \\ -0.5160 & 3.9194 \\ 4.2116 & -4.4922 \\ 3.9697 & 3.6211 \end{pmatrix}$$

$$net.LW\{3,2\}=\begin{pmatrix} -0.8095 & -0.5148 & -0.2317 & -0.8009 & 0.4658 & -0.5111 & -0.4008 & 0.7796 \\ -0.0328 & 0.6355 & 0.7744 & 0.3662 & -1.0813 & 0.9342 & -0.0122 & 1.5009 \\ 1.1926 & -0.0574 & -0.5341 & -0.5357 & 1.2538 & 0.0275 & -0.2298 & 3.7948 \\ -0.7832 & -0.3594 & -0.3250 & -1.1404 & 1.8516 & -0.5689 & 1.1293 & -1.1276 \\ -0.4821 & -0.7400 & 0.5412 & 0.3868 & -0.7215 & -0.8559 & -1.0796 & 0.2112 \\ -1.1320 & 0.2109 & 0.3646 & 0.4452 & -0.0753 & 0.1154 & 1.8460 & -2.0687 \end{pmatrix}$$

$$net.LW\{4,3\}=\begin{pmatrix} -0.9480 & 0.3208 & 0.9469 & -1.3324 & 0.0821 & -2.0665 \\ 0.5514 & 1.6292 & 0.2851 & -1.9421 & 0.0237 & 3.2556 \\ 0.6668 & -0.0409 & -0.4016 & 0.9433 & -1.2022 & 1.1777 \\ -1.0434 & -0.4636 & 3.7909 & 0.9018 & 0.2180 & -0.6989 \\ 0.8968 & 1.2777 & -1.6009 & -2.8170 & -1.1197 & 0.3627 \\ -0.5552 & -0.0718 & 2.2028 & -2.0710 & -0.3733 & 0.3461 \end{pmatrix}$$

$$net.LW\{5,4\}=\begin{pmatrix} -2.2540 & -2.6543 & 0.4038 & 0.8394 & 1.9117 & 1.1293 \end{pmatrix}$$

$$net.b\{1\}=\begin{pmatrix} -0.3650 \\ 0.0491 \end{pmatrix}$$

$$net.b\{2\}=\begin{pmatrix} -3.9600 \\ -2.8285 \\ 1.8087 \\ 0.6783 \\ 1.0615 \\ -1.2843 \\ 2.9268 \\ 2.4578 \end{pmatrix}, \; net.b\{3\}=\begin{pmatrix} 1.6354 \\ 0.6917 \\ -0.8192 \\ -0.6667 \\ -1.3231 \\ -1.3526 \end{pmatrix}, \; net.b\{4\}=\begin{pmatrix} 1.1154 \\ -0.7610 \\ -0.7228 \\ -0.7416 \\ 0.9130 \\ 1.4628 \end{pmatrix}, \; net.b\{5\}=\begin{pmatrix} 0.1207 \end{pmatrix}$$

Appendix B

$$\text{net.IW}\{1,1\}=\begin{pmatrix} 0.1248 & -0.0483 \\ -0.0075 & -0.2749 \end{pmatrix}, \qquad \text{net.LW}\{2,1\}=\begin{pmatrix} 3.8025 & 2.3630 \\ 1.6265 & -4.7208 \\ -2.2509 & -4.7286 \\ -3.2818 & 2.0771 \\ 3.1377 & 3.8890 \\ -2.1273 & -3.4451 \\ 1.6531 & 4.7484 \\ 1.9326 & -3.7690 \\ 4.6089 & -2.2740 \end{pmatrix}$$

net.LW{3,2}=

$$\begin{pmatrix} 0.7514 & -0.4912 & -1.0889 & 0.3434 & 1.1038 & -0.9175 & 0.8908 & 0.3068 & 0.3650 \\ -1.4192 & -0.8704 & -0.0522 & -0.9774 & -0.1693 & 0.2707 & 0.0894 & 0.3571 & -0.2828 \\ -0.5764 & 0.1489 & 1.7956 & -0.5783 & -1.0971 & -1.0405 & 0.6831 & -0.2026 & 1.7464 \\ -0.6317 & 1.4883 & 0.2788 & 0.2673 & -0.6555 & 1.0704 & 0.5856 & -0.2590 & 0.1436 \\ -0.5818 & 0.0870 & -1.2940 & 0.1057 & -1.5061 & 0.2616 & 2.5800 & -0.5045 & -0.0864 \\ 0.1073 & 1.0247 & 1.1220 & 0.1008 & -0.2101 & 0.8395 & 0.4734 & 0.6511 & 0.5855 \end{pmatrix}$$

$$\text{net.LW}\{4,3\}=\begin{pmatrix} 1.1395 & -0.2897 & 1.3146 & -0.7882 & 0.4975 & -0.4673 \\ -0.0919 & 1.3770 & 0.5461 & 0.7774 & -0.2470 & 0.7592 \\ 0.5938 & -1.2645 & -1.7760 & -0.5883 & 0.1816 & -0.5198 \\ 0.4472 & 1.6227 & -1.4009 & 0.5348 & -0.0590 & 1.6327 \\ 0.3676 & -0.4104 & 1.2456 & -1.2711 & -0.7957 & -0.5633 \\ 1.2604 & -0.7418 & -0.6204 & 0.0955 & -2.5943 & -0.1707 \end{pmatrix}$$

$$\text{net.LW}\{5,4\}=\begin{pmatrix} 0.1648 & 1.0649 & 0.6000 & -0.7075 & 0.1210 & -0.0740 \end{pmatrix}$$

$$\text{net.b}\{1\}=\begin{pmatrix} -2.6633 \\ 1.0054 \end{pmatrix}, \ \text{net.b}\{2\}=\begin{pmatrix} -3.9182 \\ -1.5714 \\ 1.4414 \\ 2.3693 \\ 0.1113 \\ -1.4587 \\ 2.7554 \\ 3.1627 \\ 3.1959 \end{pmatrix}, \ \text{net.b}\{3\}=\begin{pmatrix} -1.5904 \\ 1.0169 \\ 0.2069 \\ -0.4173 \\ -1.2427 \\ 1.8694 \end{pmatrix}, \ \text{net.b}\{4\}=\begin{pmatrix} -2.3907 \\ 0.8522 \\ -0.5357 \\ 1.0274 \\ 1.2204 \\ 1.8097 \end{pmatrix}$$

$$\text{net.b}\{5\}=\begin{pmatrix} 0.4067 \end{pmatrix}$$

Appendix C

$$\text{net.IW}\{1,1\}=\begin{pmatrix} -0.0038 & 0.0766 \\ -0.1274 & -0.0339 \end{pmatrix}, \qquad \text{net.LW}\{2,1\}=\begin{pmatrix} 2.6906 & 3.1115 \\ 2.7690 & 3.0472 \\ -0.2357 & -3.5886 \\ -6.1560 & -1.5610 \\ 2.8746 & 4.3798 \\ 0.3877 & 4.4910 \\ 5.4678 & -3.7740 \\ 4.5420 & 2.9780 \end{pmatrix}$$

$$\text{net.LW}\{3,2\}=$$
$$\begin{pmatrix} -0.6232 & -0.3284 & -0.3816 & -2.4284 & 0.7919 & -0.3223 & -1.4376 & 4.3457 \\ -0.4671 & 0.1984 & 1.1961 & 0.7620 & 0.0316 & 0.8532 & 2.0583 & 0.7098 \\ 0.2886 & -0.8896 & -0.2670 & -0.5847 & -0.4071 & -1.0655 & 1.9955 & 2.4621 \\ -2.6208 & -2.5601 & -0.7476 & -1.3935 & 0.4563 & 0.1654 & -0.5779 & -4.1692 \\ -0.5504 & -0.1933 & 0.4259 & 0.1907 & 0.1163 & -1.7650 & 0.4125 & -3.2289 \\ -0.4528 & 0.6073 & 0.3382 & 1.7211 & -0.2759 & 0.8575 & 2.5504 & -0.3690 \end{pmatrix}$$

$$\text{net.LW}\{4,3\}\begin{pmatrix} -0.8104 & -0.2231 & 0.2690 & 0.0916 & 1.4115 & -1.0588 \\ -2.1483 & 0.9570 & 1.4299 & -0.2473 & -1.7624 & 1.1028 \\ 1.6564 & -0.9850 & -0.3453 & 1.2319 & 0.0940 & 1.0272 \\ 0.3666 & 0.2376 & 1.9793 & -1.1670 & 0.2884 & -1.3334 \\ 1.6122 & -0.2795 & -2.0286 & -2.7499 & -2.7697 & -0.2563 \\ -0.5250 & -0.2465 & 3.1180 & -1.4866 & -0.8357 & -0.0922 \end{pmatrix}$$

$$\text{net.LW}\{5,4\}=\begin{pmatrix} -1.9627 & -2.2284 & -2.9394 & -1.9775 & -0.2732 & 1.0151 \end{pmatrix}$$

$$\text{net.b}\{1\}=\begin{pmatrix} -0.9170 \\ 0.4899 \end{pmatrix}, \qquad \text{net.b}\{2\}=\begin{pmatrix} -3.6318 \\ -2.3421 \\ 0.7712 \\ -0.4517 \\ 2.3715 \\ -1.3364 \\ 1.7903 \\ 4.1891 \end{pmatrix} \qquad \text{net.b}\{3\}=\begin{pmatrix} 1.4492 \\ 1.1254 \\ 0.0958 \\ 1.0917 \\ -1.1397 \\ -2.1010 \end{pmatrix}, \qquad \text{net.b}\{4\}=\begin{pmatrix} 2.0725 \\ -1.8718 \\ -1.0936 \\ -1.7491 \\ 0.4900 \\ 1.1316 \end{pmatrix}$$

$$\text{net.b}\{5\}=\begin{pmatrix} -1.8464 \end{pmatrix}$$

REFERENCES

[1] Singh, G., Sengupta, K, and Jain, P.L., *Phys. Rev. C* **41**, 999 (1990).

[2] Gupta, S.D., et al, *Adv. Nucl. Phys.* **26**, 89 (2001) ; Bondrof, P.J., et al., *Phys. Rep.* **257**, 133 (1995); and reference therein.

[3] Glauber, R. J., *Lectures in Theoretical Physics*, New York: Wiley-Interscience, 1959.

[4] Islam, M. M., Luddy, R. J., Prokudin, A. V., *Mod. Phys. Lett.* **18**, 743 (2003); hep-ph/0210437.

[5] Abu-Ibrahim, B., Suzuki, Y., *Nucl.Phys.* **A728,** 118-132 (2003) - Arellano, H. F., Geramb, H. V., *Phys. Rev.*, **C66** (2002) 024602.

[6] Thomas D. Cohen, Daniel C. Dakin, Phys.Rev. C68 (2003) 017001.

[7] B. Davids, S. Typel, Phys.Rev. C68 (2003) 045802.

[8]. Hassan, N. M., El-Harby, N., Hussein, M. T., *APH N.S. Heavy Ion Physics* **12** 33(2000).

[9] Braun, M. A., *Phys. Lett.* **B 483,** 115 (2000).

[10] Hussein, M. T., Rabea, A., El-Naghy, A., and Hassan, N.M., *Prog. Theor. Phys.***93** 595 (1995).

[11] Klatke J.U., and Mutter, K.H., *Nucl.Phys.* **B 342**, 764 (1990).

[12] Hussein, M.T., Hassan, N.M., and Hegab, M.K., *Indian J. Phys.* **62A**, 383 (1988).

[13] Singh, V., et al., nucl-ex/0412051.

[14] Abdelsalam, A., JINR Report, EI-81-623 (1981).

[15] Babecki, J.,*Act. Phys. Pol.* **B 6**, 443 (1975).

[16] Anzon, E. V., et al., *Sov. J. Nucl. Phys.* **22**, 380 (1976).

[17] Otterlund, I., LUIP-CR-76-05 (1976).

[18] Buszew, the VI Th Conf. on High Energy Physics and Nuclear Struct. Los Alamos and Santa Fe, 1975.

[19] Cinchezn, J. et al., *Nucl. Phys.* **B 158**, 280 (1979).

[20] Baroni, G., et al., *Nucl. Phys.* **A 516,** 673 (1990).

[21] Florian, J. P., et al., Report Submitted to the Meeting of the Division of Particles and Field, Berkeley, CA (1973).

[22] Tolstov, K. D., Dubna-Frankfurt Cooperation and Comments to the Int. Conf. on Extreme States in Nucl. Sys., GDR, February, (1980).

[23] Haykin, S., *Neural Network: A comprehensive foundation*, 2nd Edition, New Jersey : Prentice Hall, 2002.

[24] Dias, F. M., et al., *Eng. App. of Artificial Intelligence* **19**, 1 (2006).

[25] Hagan, M. T., Menhaj, M.B., *IEEE Transactions on neural networks* **5**, 989 (1994).